

Association of plasma and cortical amyloid beta is modulated by *APOE* $\epsilon 4$ status

Shanker Swaminathan^{a,b}, Shannon L. Risacher^a, Karmen K. Yoder^a, John D. West^a, Li Shen^{a,c},
Sungeun Kim^{a,c}, Mark Inlow^{a,d}, Tatiana Foroud^{a,b,c}, William J. Jagust^e, Robert A. Koeppe^f,
Chester A. Mathis^g, Leslie M. Shaw^h, John Q. Trojanowski^h, Holly Soaresⁱ, Paul S. Aisen^j,
Ronald C. Petersen^k, Michael W. Weiner^l, Andrew J. Saykin^{a,b,c,*}; for the Alzheimer's Disease
Neuroimaging Initiative[†]

^aCenter for Neuroimaging, Department of Radiology and Imaging Sciences,
Indiana University School of Medicine, Indianapolis, IN, USA

^bDepartment of Medical and Molecular Genetics, Indiana University School of Medicine, Indianapolis, IN, USA

^cCenter for Computational Biology and Bioinformatics, Indiana University School of Medicine, Indianapolis, IN, USA

^dDepartment of Mathematics, Rose-Hulman Institute of Technology, Terre Haute, IN, USA

^eHelen Wills Neuroscience Institute, University of California at Berkeley, Berkeley, CA, USA

^fDivision of Nuclear Medicine, Department of Radiology, University of Michigan, Ann Arbor, MI, USA

^gDepartment of Radiology, University of Pittsburgh, Pittsburgh, PA, USA

^hDepartment of Pathology and Laboratory Medicine, University of Pennsylvania School of Medicine, Philadelphia, PA, USA

ⁱBristol Myers Squibb Co., Wallingford, CT, USA

^jDepartment of Neurosciences, University of California at San Diego, San Diego, CA, USA

^kDepartment of Neurology, Mayo Clinic and Foundation, Rochester, MN, USA

^lDepartment of Veterans Affairs Medical Center, Center for Imaging of Neurodegenerative Diseases, San Francisco, CA, USA

Abstract

Background: Apolipoprotein E (*APOE*) $\epsilon 4$ allele's role as a modulator of the relationship between soluble plasma amyloid beta ($A\beta$) and fibrillar brain $A\beta$ measured by Pittsburgh compound B positron emission tomography ($[^{11}C]PiB$ PET) has not been assessed.

Methods: Ninety-six Alzheimer's Disease Neuroimaging Initiative participants with $[^{11}C]PiB$ scans and plasma $A\beta_{1-40}$ and $A\beta_{1-42}$ measurements at the time of PET scanning were included. Regional and voxelwise analyses of $[^{11}C]PiB$ data were used to determine the influence of *APOE* $\epsilon 4$ allele on association of plasma $A\beta_{1-40}$, $A\beta_{1-42}$, and $A\beta_{1-40}/A\beta_{1-42}$ with $[^{11}C]PiB$ uptake.

Results: In *APOE* $\epsilon 4-$ but not $\epsilon 4+$ participants, positive relationships between plasma $A\beta_{1-40}/A\beta_{1-42}$ and $[^{11}C]PiB$ uptake were observed. Modeling the interaction of *APOE* and plasma $A\beta_{1-40}/A\beta_{1-42}$ improved the explained variance in $[^{11}C]PiB$ binding compared with using *APOE* and plasma $A\beta_{1-40}/A\beta_{1-42}$ as separate terms.

Conclusions: The results suggest that plasma $A\beta$ is a potential Alzheimer's disease biomarker and highlight the importance of genetic variation in interpretation of plasma $A\beta$ levels.

© 2014 The Alzheimer's Association. All rights reserved.

Keywords:

Alzheimer's disease; Mild cognitive impairment; Alzheimer's Disease Neuroimaging Initiative; Amyloid beta; Plasma amyloid beta; Positron emission tomography; Pittsburgh compound B; Apolipoprotein E

[†]Data used in preparation of this article were obtained from the Alzheimer's Disease Neuroimaging Initiative (ADNI) database (<http://adni.loni.ucla.edu>). As such, the investigators within the ADNI contributed to the design and implementation of ADNI and/or provided data, but did not participate in analysis or writing the report. A complete listing

of ADNI investigators can be found at http://adni.loni.ucla.edu/wp-content/uploads/how_to_apply/ADNI_Acknowledgement_List.pdf.

*Corresponding author. Tel.: +317-963-7501; Fax: +317-963-7547.

E-mail address: asaykin@iupui.edu

1. Introduction

Alzheimer's disease (AD) is the most common type of dementia, affecting an estimated 5.4 million Americans [1]. Currently, there are no treatments that can stop its progression. However, worldwide research efforts are being conducted to identify improved methods to prevent, diagnose, and treat this disease [1]. Objective measures of biological or pathogenic processes, called biomarkers, can help in the evaluation of disease risk or prognosis. To date, no reliable biomarkers for AD in peripheral blood have been found [2].

AD is characterized by declining memory and cognition. Amnesic mild cognitive impairment (MCI) is a clinical condition thought to be a prodromal stage of AD, in which individuals have cognitive problems not normal for their age, but are not severe enough to interfere significantly with daily life activities. An estimated 14% to 18% of individuals 70 years and older have MCI, and approximately 10% to 15% of these individuals with MCI will progress to dementia, mostly AD, each year [3,4].

Accumulation of amyloid beta ($A\beta$) fragments into amyloid plaques in the brain is one of the defining pathologies of AD. Attempts to monitor the presence and/or progression of amyloid deposition have focused primarily on measurements of $A\beta$ in the brain and cerebrospinal fluid (CSF). The level of CSF $A\beta_{1-42}$ has been shown to be a sensitive biomarker for detection and diagnosis of AD [5–7]. Positron emission tomography (PET) imaging techniques with ligands such as Pittsburgh compound B ($[^{11}C]PiB$) [8] and $[^{18}F]$ florbetapir [9,10], which bind fibrillar $A\beta$ plaques with high affinity, are being studied for their efficacy in predicting and diagnosing AD and have shown some promise [11–13].

Identifying a peripheral biomarker of central $A\beta$ deposition may help in the diagnosis and treatment of the disease at earlier stages. Measuring soluble $A\beta$ levels in plasma would provide an easy method to study $A\beta$ because the procedure is minimally invasive and relatively inexpensive. The utility of plasma $A\beta$ as a potential AD biomarker has been assessed in previous studies, but the results have been inconsistent [14–17]. Possible reasons for the inconsistent results could be the use of different enzyme-linked immunosorbent assays and platforms, and timing of sample collection in relation to the stage of disease progression. Therefore, additional studies are needed to characterize more fully the utility of plasma $A\beta$ measures as sensitive and effective biomarkers of AD.

Genetic factors, such as the apolipoprotein E (*APOE*) gene, may play a role in amyloid accumulation and the development of AD. The *APOE* gene is expressed as three variants: $\epsilon 2$, $\epsilon 3$, and $\epsilon 4$. The *APOE* $\epsilon 4$ allele is the strongest genetic risk factor of late-onset AD and confers a dose-dependent increase in AD risk of approximately fourfold in carriers compared with noncarriers [18–20]. The $\epsilon 4$ allele is also associated with increased fibrillar $A\beta$ [21] and decreased soluble plasma $A\beta_{1-42}$ [22] in a dose-

dependent manner. The *APOE* gene codes for the apoE protein, which is essential for maintaining blood–brain barrier (BBB) integrity [23]. The apoE4 form of the apoE protein, coded for by the $\epsilon 4$ allele, has been associated with reduced $A\beta$ clearance from the brain [24] and plasma [25], and with impaired tight junction integrity [26].

To our knowledge, only four studies have investigated the relationship of soluble plasma $A\beta$ and fibrillar brain $A\beta$ as measured by $[^{11}C]PiB$ [22,27–29]. The first study [27] did not identify any relationships between plasma $A\beta_{1-40}$ and $A\beta_{1-42}$ levels and $[^{11}C]PiB$ binding. In the other studies, inverse correlations were observed between plasma $A\beta_{1-42}$ and $[^{11}C]PiB$ uptake [22,28] and between $A\beta_{1-42}/A\beta_{1-40}$ and brain amyloid [28,29]. However, none of these studies examined the potential influence of genetic variation in AD-related genes (e.g., *APOE* $\epsilon 4$) on relationships between peripheral and central markers of $A\beta$. Furthermore, these studies only included regional measures of $[^{11}C]PiB$ uptake rather than voxel-based mapping across the whole brain, which may have limited the findings because extracting information from spatially large regions may dilute or obscure relevant results that are spatially constrained.

We studied the associations among $[^{11}C]PiB$ brain uptake, soluble plasma $A\beta$ measurements, and *APOE* $\epsilon 4$ genotype status in 96 participants from the Alzheimer's Disease Neuroimaging Initiative (ADNI) to determine whether the relationship of soluble plasma $A\beta$ measures and fibrillar brain amyloid was influenced by *APOE* $\epsilon 4$ status. First, we used the average regional $[^{11}C]PiB$ uptake across four target brain regions known to have amyloid deposition in AD as a quantitative phenotype in regression analyses. We then conducted whole-brain, voxelwise regression analyses to identify spatially specific clusters in which the *APOE* $\epsilon 4$ genotype modulated the association of plasma and brain PET measurements of $A\beta$.

2. Methods

2.1. Alzheimer's Disease Neuroimaging Initiative

Data used in the preparation of this report were obtained from the ADNI database (<http://adni.loni.ucla.edu>). The ADNI was initiated in 2003 as a \$60 million, 5-year public–private partnership by the National Institute on Aging, the National Institute of Biomedical Imaging and Bioengineering, the Food and Drug Administration, private pharmaceutical companies, and nonprofit organizations. The primary goal of the ADNI is to test whether serial magnetic resonance imaging (MRI), PET, other biological markers, genetics, and clinical and neuropsychological assessments can be combined to detect and measure the progression of MCI and early AD. Determining sensitive and specific markers of very early AD progression can aid researchers and clinicians in developing new treatments and monitoring their effectiveness, as well as lessen the time and cost of clinical trials.

Michael W. Weiner, MD, Veterans Affairs Medical Center and University of California at San Francisco, is the principal investigator of this initiative. ADNI is the result of the efforts of many co-investigators from a broad range of academic institutions and private corporations. As part of the initial phase of ADNI, more than 800 participants, age 55 to 90 years, were recruited from more than 50 sites across the United States and Canada, including approximately 200 cognitively healthy older individuals (healthy control subjects [HCs]) to be monitored for 3 years, 400 people with MCI to be monitored for 3 years, and 200 people with early AD to be monitored for 2 years. Further information about ADNI can be found in work by Weiner and colleagues [30] and at <http://www.adni-info.org>.

The study was conducted after institutional review board approval at each site. Written informed consent was obtained from all study participants or their authorized representatives.

2.2. Participants

Data from 96 participants in the ADNI cohort were evaluated. Participant selection was based on the availability of the following data: [¹¹C]PiB PET scans, plasma measurements of Aβ_{1–40} and Aβ_{1–42} at time of PET scan, and APOE ε4 genotype data. At the time of PET scan, 22 participants were in the AD group, 52 in the MCI group, and 22 in the HC group. The participants included 89 non-Hispanic whites, two non-Hispanic blacks, two non-Hispanic Asians, two Hispanic whites, and 1 white participant of unknown ethnicity. Additional demographic information about the included sample is presented in Table 1.

2.2.1. [¹¹C]PiB PET image data

For all participants, PET data consisted of each participant's initial [¹¹C]PiB scan in the ADNI longitudinal imaging protocol. Initial scans were acquired at either the participant's baseline visit, 12-month visit, or 24-month

visit (Table 1). Methods for the acquisition and processing of [¹¹C]PiB PET scans for the ADNI sample have been described elsewhere [31,32]. The PET data used in the current study were what was available as of October 2010. The ADNI database includes normalized whole-brain [¹¹C]PiB images as well as normalized regional [¹¹C]PiB average uptake values extracted from anatomically defined regions of interest (ROIs). Both pre-existing ROI data and whole-brain [¹¹C]PiB images were downloaded and analyzed in the current study. Regional [¹¹C]PiB standardized uptake value ratios from four ROIs (anterior cingulate, frontal cortex, parietal cortex, and precuneus) were averaged and used as a quantitative phenotype, referred to as average regional [¹¹C]PiB uptake. This metric has been used previously to classify participants as positive or negative for amyloid deposition [32].

The whole-brain [¹¹C]PiB PET images evaluated in the current study were preprocessed (PIB Coreg, Avg, Std Img and Vox Size, Uniform Resolution), as described previously described [32]. Briefly, the images were set to a standard orientation and voxel size, intensity normalized using a cerebellar gray matter (GM) ROI, and smoothed to a common resolution of 8 mm full-width at half maximum. These preprocessed scans were downloaded in Neuroimaging Informatics Technology Initiative format from the ADNI scan repository (<http://adni.loni.ucla.edu>) and processed further using Statistical Parametric Mapping [33] version 5 (SPM5; <http://www.fil.ion.ucl.ac.uk/spm/>) implemented via MATLAB v7.1.0 (MathWorks, Natick, MA) [34]. Specifically, for all participants, 1.5-T T1-weighted three-dimensional magnetization-prepared rapid acquisition gradient echo magnetic resonance (MR) images [35] acquired at the same time point as the [¹¹C]PiB scans were also downloaded from the ADNI site (<http://adni.loni.ucla.edu>). The preprocessed [¹¹C]PiB PET image of each participant was coregistered to their corresponding MR image. PET and MR data were then

Table 1
Sample characteristics

Characteristic	AD (n = 22)	MCI (n = 52)	HC (n = 22)	P value*
Initial [¹¹ C]PiB scans at baseline/12-month/24-month visit	3/13/6	11/36/5	0/20/2	.034
Age at time of scan, years; mean ± SD	74.06 ± 9.09	75.35 ± 7.93	77.14 ± 6.17	.428
Sex, n; male/female	15/7	35/17	14/8	.940
Education, years; mean ± SD	15.73 ± 3.04	16.31 ± 2.65	15.50 ± 3.32	.492
Handedness, n; right/left	20/2	48/4	17/5	.165
APOE ε4 status, n; ε4–/ε4+	8/14	24/28	16/6	.039
Average regional [¹¹ C]PiB uptake [†] , mean ± SD	2.01 ± 0.31	1.81 ± 0.44	1.56 ± 0.34	.001
Plasma Aβ _{1–40} , pg/mL; mean ± SD	160.99 ± 47.89	171.56 ± 48.60	168.75 ± 36.57	.666
Plasma Aβ _{1–42} , pg/mL; mean ± SD	36.05 ± 9.19	40.81 ± 12.48	41.93 ± 9.06	.160
Plasma Aβ _{1–40} /Aβ _{1–42} , mean ± SD	4.53 ± 1.20	4.38 ± 1.19	4.11 ± 0.81	.440

Abbreviations: AD, Alzheimer's disease; MCI, mild cognitive impairment; HC, healthy control participant; PiB, Pittsburgh compound B; SD, standard deviation; APOE, apolipoprotein E; Aβ, amyloid beta.

*For categorical variables, Pearson χ² was used to compute the P value. For continuous variables, one-way analysis of variance was used to compute the P value.

[†]Average regional [¹¹C]PiB uptake is the average of [¹¹C]PiB uptake values from four brain regions—anterior cingulate, frontal cortex, parietal cortex, and precuneus—normalized to cerebellum.

spatially normalized to Montreal Neurological Institute (MNI) space using transformation parameters estimated from the SPM segmentation algorithm [36]. These spatially normalized PET images were used for the whole-brain voxelwise analysis.

2.2.2. Plasma A β data

Plasma A β_{1-40} and A β_{1-42} levels for participants with [^{11}C]PiB PET scans from the same time point that the PET data were acquired were obtained from the ADNI database. The methods for the collection, measurement, and quality control of plasma samples have been described previously [22,37].

2.2.3. APOE $\epsilon 4$ genotyping

The APOE $\epsilon 4$ status of all participants was determined by two single nucleotide polymorphisms (rs429358 and rs7412), as described previously [38]. Participants were classified as APOE $\epsilon 4-$ (absence of the $\epsilon 4$ allele) or APOE $\epsilon 4+$ (presence of the $\epsilon 4$ allele).

2.3. Statistical analyses

The influence of APOE $\epsilon 4$ status on the association between plasma A β and average regional [^{11}C]PiB uptake was assessed in R version 2.10.0 [39] and SAS 9.3 (SAS Institute Inc., Cary, NC) using the following regression models:

1. Average regional [^{11}C]PiB uptake = Plasma A β_{1-40} + APOE $\epsilon 4$ status + (Plasma A β_{1-40} \times APOE $\epsilon 4$ status)
2. Average regional [^{11}C]PiB uptake = Plasma A β_{1-42} + APOE $\epsilon 4$ status + (Plasma A β_{1-42} \times APOE $\epsilon 4$ status)
3. Average regional [^{11}C]PiB uptake = Plasma A $\beta_{1-40}/\text{A}\beta_{1-42}$ + APOE $\epsilon 4$ status + (Plasma A $\beta_{1-40}/\text{A}\beta_{1-42}$ \times APOE $\epsilon 4$ status)

Models with significant interactions between plasma A β and APOE $\epsilon 4$ status on average regional [^{11}C]PiB uptake were identified. For these models, the variance in average regional [^{11}C]PiB uptake explained by different terms in the model was determined using the following regression models:

1. Variance in average regional [^{11}C]PiB uptake explained by plasma A β term alone:
Average regional [^{11}C]PiB uptake = Plasma A β
2. Variance in average regional [^{11}C]PiB uptake explained by APOE $\epsilon 4$ status term alone:
Average regional [^{11}C]PiB uptake = APOE $\epsilon 4$ status
3. Variance in average regional [^{11}C]PiB uptake explained by plasma A β and APOE $\epsilon 4$ status terms together:
Average regional [^{11}C]PiB uptake = Plasma A β + APOE $\epsilon 4$ status

4. Variance in average regional [^{11}C]PiB uptake explained by plasma A β , APOE $\epsilon 4$ status, and (plasma A β \times APOE $\epsilon 4$ status) terms together:

Average regional [^{11}C]PiB uptake = Plasma A β + APOE $\epsilon 4$ status + (Plasma A β \times APOE $\epsilon 4$ status)

The influence of APOE $\epsilon 4$ status on the association between plasma A β and [^{11}C]PiB uptake was assessed further in whole-brain voxelwise analyses in SPM5 using the following regression models:

1. Voxel [^{11}C]PiB uptake = Plasma A β_{1-40} + APOE $\epsilon 4$ status + (Plasma A β_{1-40} \times APOE $\epsilon 4$ status)
2. Voxel [^{11}C]PiB uptake = Plasma A β_{1-42} + APOE $\epsilon 4$ status + (Plasma A β_{1-42} \times APOE $\epsilon 4$ status)
3. Voxel [^{11}C]PiB uptake = Plasma A $\beta_{1-40}/\text{A}\beta_{1-42}$ + APOE $\epsilon 4$ status + (Plasma A $\beta_{1-40}/\text{A}\beta_{1-42}$ \times APOE $\epsilon 4$ status)

In the voxelwise analyses, an explicit GM mask was used to restrict analyses to GM regions. Significant interactions were determined using a voxel-level threshold of $P < .005$ (uncorrected) and a cluster-level threshold of $k \geq 200$ contiguous voxels to achieve cluster-level uncorrected $P < .05$. Clusters identified in the left or right cerebellum were not considered because the [^{11}C]PiB PET images had been intensity normalized using a cerebellar GM ROI. Voxels at which significant relationships existed were displayed on a three-dimensional-rendered brain. The MNI coordinates of voxels that were peak maxima and local maxima (voxels > 4 mm apart) in each cluster were converted to Talairach coordinates, and queried in Talairach Client v2.4.2 [40,41] software to determine the associated anatomic labels. Random field theory corrected P values (P_{corr}) were used to identify significant clusters. Mean [^{11}C]PiB uptake from each significant cluster was extracted for all participants, and their distribution in APOE $\epsilon 4-$ and APOE $\epsilon 4+$ participants was further examined in R version 2.10.0 and SAS 9.3. We then evaluated further the relationship of mean [^{11}C]PiB uptake from the biggest and most significant cluster and plasma A β levels. The variance in mean [^{11}C]PiB uptake extracted from the significant cluster explained by different terms in the model was determined using the following regression models:

1. Variance in mean [^{11}C]PiB uptake from the significant cluster explained by plasma A β term alone:
Mean [^{11}C]PiB uptake from the significant cluster = Plasma A β
2. Variance in mean [^{11}C]PiB uptake from the significant cluster explained by APOE $\epsilon 4$ status term alone:
Mean [^{11}C]PiB uptake from the significant cluster = APOE $\epsilon 4$ status
3. Variance in mean [^{11}C]PiB uptake from the significant cluster explained by plasma A β and APOE $\epsilon 4$ status terms together:

Mean [^{11}C]PiB uptake from the significant cluster = Plasma A β + *APOE* $\epsilon 4$ status

4. Variance in mean [^{11}C]PiB uptake from the significant cluster explained by plasma A β , *APOE* $\epsilon 4$ status, and (plasma A β \times *APOE* $\epsilon 4$ status) terms together:

Mean [^{11}C]PiB uptake from the significant cluster = Plasma A β + *APOE* $\epsilon 4$ status + (Plasma A β \times *APOE* $\epsilon 4$ status)

3. Results

We first investigated the influence of *APOE* $\epsilon 4$ status on the association between plasma A β and average regional [^{11}C]PiB uptake. No significant interactions between plasma A β_{1-40} and *APOE* $\epsilon 4$ status or between plasma A β_{1-42} and *APOE* $\epsilon 4$ status were observed on average regional [^{11}C]PiB uptake. However, a significant interaction between plasma A $\beta_{1-40}/\text{A}\beta_{1-42}$ and *APOE* $\epsilon 4$ status ($P = .025$) on average regional [^{11}C]PiB uptake was observed. Inclusion of age at time of scan and gender as covariates did not alter this finding. *APOE* $\epsilon 4$ genotype status ($\epsilon 4-$ or $\epsilon 4+$) conferred different patterns of association between plasma

A $\beta_{1-40}/\text{A}\beta_{1-42}$ and average regional [^{11}C]PiB uptake. Specifically, in the *APOE* $\epsilon 4-$ participants, there was a positive relationship between plasma A $\beta_{1-40}/\text{A}\beta_{1-42}$ and average regional [^{11}C]PiB uptake (slope = 0.162, $P = .008$, $r^2 = 0.141$; Fig. 1A). However, this relationship did not exist in the *APOE* $\epsilon 4+$ participants (slope = -0.005 ; $P = .901$; $r^2 < 0.001$; Fig. 1B). The *APOE* $\epsilon 4$ status and plasma A $\beta_{1-40}/\text{A}\beta_{1-42}$ terms explained 17% and 6% of variation in average regional [^{11}C]PiB uptake, respectively. The two terms together explained 19% of variation in average regional [^{11}C]PiB uptake. Inclusion of the (plasma A $\beta_{1-40}/\text{A}\beta_{1-42}$ \times *APOE* $\epsilon 4$ status) interaction term in the model increased the explained variance in average regional [^{11}C]PiB uptake to 24%.

To examine further the spatial extent of the potential influence of *APOE* $\epsilon 4$ status on the association of plasma A β and [^{11}C]PiB uptake, we performed whole-brain, voxelwise regression analyses. *APOE* genotype did not affect significantly the positive or negative associations between plasma A β_{1-40} and [^{11}C]PiB uptake, and between plasma A β_{1-42} and [^{11}C]PiB uptake in cerebral regions. However, *APOE* genotype significantly altered the

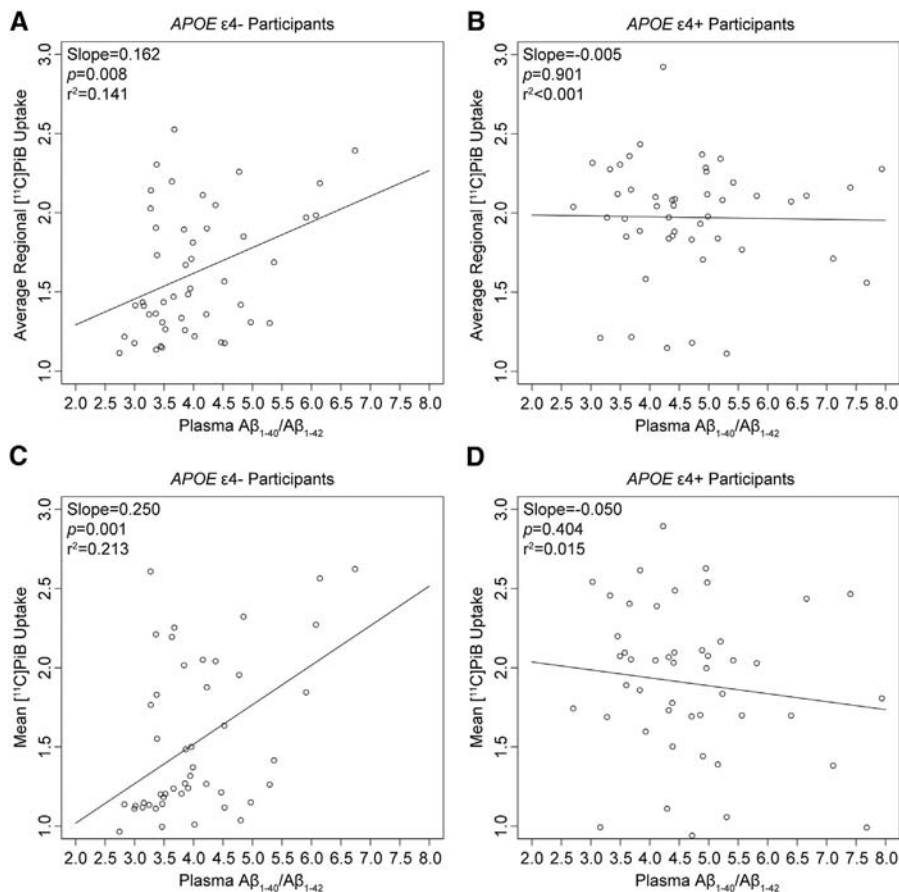


Fig. 1. (A–D) Scatterplots of plasma A $\beta_{1-40}/\text{A}\beta_{1-42}$ vs average regional [^{11}C]PiB uptake from the (Average regional [^{11}C]PiB uptake = Plasma A $\beta_{1-40}/\text{A}\beta_{1-42}$ + *APOE* $\epsilon 4$ status + [Plasma A $\beta_{1-40}/\text{A}\beta_{1-42}$ \times *APOE* $\epsilon 4$ status]) model (A and B), and plasma A $\beta_{1-40}/\text{A}\beta_{1-42}$ vs mean [^{11}C]PiB uptake from the cluster identified in the (Voxel [^{11}C]PiB uptake = Plasma A $\beta_{1-40}/\text{A}\beta_{1-42}$ + *APOE* $\epsilon 4$ status + [Plasma A $\beta_{1-40}/\text{A}\beta_{1-42}$ \times *APOE* $\epsilon 4$ status]) model (C and D). A β , amyloid beta; PiB, Pittsburgh compound B; *APOE*, apolipoprotein E.

negative correlation of plasma $A\beta_{1-40}/A\beta_{1-42}$ and [^{11}C]PiB uptake in a significant cluster in the left inferior frontal gyrus (MNI peak coordinates: $x = -40$, $y = 18$, $z = -6$; $k = 6152$ voxels; cluster-level $P_{\text{corr}} < .001$; Fig. 2 and Table 2). Similar to the data from the average regional [^{11}C]PiB uptake analysis, there was a positive relationship between plasma $A\beta_{1-40}/A\beta_{1-42}$ and mean [^{11}C]PiB uptake from the inferior frontal gyral cluster in the $APOE \epsilon 4-$ participants (slope = 0.250, $P = .001$, $r^2 = 0.213$; Fig. 1C), but not in the $APOE \epsilon 4+$ participants (slope = -0.050 , $P = .404$, $r^2 = 0.015$; Fig. 1D). Inclusion of age at time of scan and gender as covariates again did not alter this finding. The $APOE \epsilon 4$ status and plasma $A\beta_{1-40}/A\beta_{1-42}$ terms by themselves explained 13% and 4% of variation in mean [^{11}C]PiB uptake from the significant cluster, respectively. The two terms together explained 14% of variation in mean [^{11}C]PiB uptake from the significant cluster. Inclusion of the (plasma $A\beta_{1-40}/A\beta_{1-42} \times APOE \epsilon 4$ status) interaction term along with the two terms in the model increased the variance explained in mean [^{11}C]PiB uptake from the significant cluster to 23%. No clusters were identified when considering the positive correlation of plasma $A\beta_{1-40}/A\beta_{1-42}$ and [^{11}C]PiB uptake.

4. Discussion

The investigation of $A\beta$ species in plasma offers advantages over conventional methods for measuring $A\beta$ levels in the brain and CSF. Obtaining and analyzing plasma samples is relatively inexpensive, minimally invasive, and can be performed easily at multiple time points. Therefore, a plasma-based biomarker for early detection and diagnosis of AD would be ideal. In the ADNI cohort, a strong association has been observed between CSF $A\beta_{1-42}$ and fibrillar brain $A\beta$ (indexed with [^{11}C]PiB) [31], whereas a weak but significant association has been observed between CSF $A\beta_{1-42}$ and soluble plasma $A\beta_{1-42}$ [37]. However, the association between soluble plasma $A\beta$ and fibrillar brain $A\beta$ is unclear.

We investigated the relationship of soluble plasma $A\beta$ ($A\beta_{1-40}$, $A\beta_{1-42}$, and $A\beta_{1-40}/A\beta_{1-42}$), $APOE \epsilon 4$ status, and fibrillar brain $A\beta$ (indexed with [^{11}C]PiB) in the ADNI cohort. In two types of analytical approaches, $APOE \epsilon 4$ genotype status had a significant effect on the relationship between plasma $A\beta_{1-40}/A\beta_{1-42}$ and [^{11}C]PiB uptake. Specifically, a positive relationship between plasma $A\beta_{1-40}/A\beta_{1-42}$ and [^{11}C]PiB signal was observed in $APOE \epsilon 4-$ participants, but not in $APOE \epsilon 4+$ participants (Fig. 1). This finding may reflect a stronger relationship between plasma $A\beta$ and accumulation of fibrillar amyloid in the brain in individuals at an earlier and/or less severe disease state (e.g., $APOE \epsilon 4-$). A recent study suggested that plasma $A\beta$ levels in cognitively stable individuals tend to increase slightly with age [15]. Cognitively normal individuals with higher plasma $A\beta$ levels are thought to be at an increased risk of progression to AD. Plasma $A\beta$ levels in individuals who go on to develop AD tend to be elevated during the prodementia stage, reach a peak, and then decrease prior to developing clinical AD symptoms. Increasing brain amyloid deposits in the later stages of disease may perhaps reduce interstitial $A\beta$ in the brain and CSF, confounding the relationship between plasma $A\beta$ and brain amyloid.

The molecular mechanism by which the $APOE \epsilon 4$ allele leads to increased risk for AD is unclear. The $APOE$ gene codes for the apoE protein, which is essential for maintaining BBB integrity [23]. Furthermore, the various apoE protein isoforms are thought to clear $A\beta$ from the brain differentially into the plasma across the BBB. In a recent study, Castellano and colleagues [24] found that mice expressing the human apoE4 protein had greater $A\beta$ concentrations in the interstitial fluid of the brain and hippocampus, and showed reduced $A\beta$ clearance from the interstitial fluid of the brain when compared with mice expressing the human apoE2 or apoE3 proteins. However, they did not find differences in $A\beta$ synthesis or amyloidogenic processing between mice expressing the different apoE protein isoforms. In another study conducted in $APOE \epsilon 2$, $\epsilon 3$, and $\epsilon 4$ knock-in and $APOE$ knock-out mice injected with lipidated recombinant apoE2, E3, and E4 proteins, Sharman and colleagues [25]

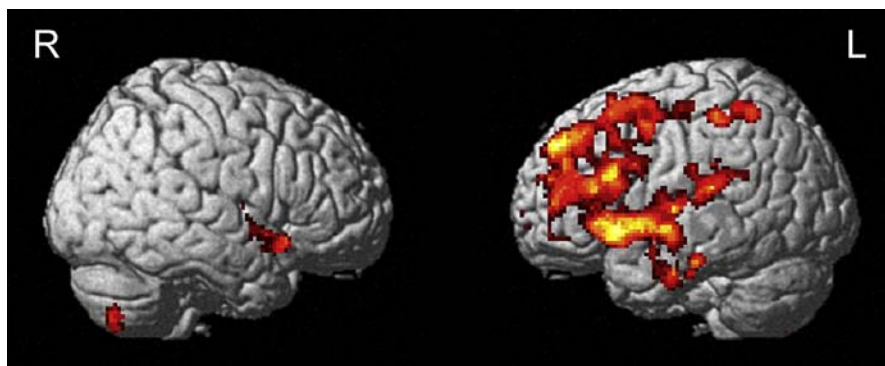


Fig. 2. Brain regions (R, right; L, left) identified in the (Voxel [^{11}C]PiB uptake = Plasma $A\beta_{1-40}/A\beta_{1-42}$ + $APOE \epsilon 4$ status + [Plasma $A\beta_{1-40}/A\beta_{1-42} \times APOE \epsilon 4$ status]) model (voxel-level threshold of $P < .005$ [uncorrected], cluster size ≥ 200 voxels). The red-to-yellow scale indicates increasing statistical significance of association. PiB, Pittsburgh compound B; $A\beta$, amyloid beta; $APOE$, apolipoprotein E.

Table 2

Brain regions identified in the (Voxel [^{11}C]PiB uptake = Plasma $\text{A}\beta_{1-40}/\text{A}\beta_{1-42}$ + $\text{APOE } \epsilon 4$ status + [Plasma $\text{A}\beta_{1-40}/\text{A}\beta_{1-42}$ \times $\text{APOE } \epsilon 4$ status]) model (voxel-level threshold of $P < .005$ [uncorrected], cluster size ≥ 200 voxels)

Region	Brodmann area	Peak value coordinates, mm			Voxel level		Cluster level		
		x	y	z	T value	$P_{\text{FWE-corr}}$	k	P_{uncorr}	P_{corr}
Left inferior frontal gyrus	BA47	-40	18	-6	3.92	.713	6152	<.001	<.001
Left superior temporal gyrus	BA22	-46	6	-4	3.85	.774			
Left middle frontal gyrus	BA6	-30	12	60	3.81	.816			
Left superior frontal gyrus	BA8	-28	20	56	3.76	.855			
Left precentral gyrus	BA4	-34	-20	52	3.68	.910			
Left insula	BA13	-42	-8	-8	3.58	.955			
Left middle frontal gyrus	BA8	-24	24	50	3.43	.990			
Left middle frontal gyrus	BA10	-36	42	14	3.40	.993			
Left middle temporal gyrus	BA21	-58	-10	-8	3.35	.996			
Left superior frontal gyrus	BA9	-18	48	34	3.29	.998			
Left inferior frontal gyrus	BA45	-50	20	20	3.24	.999			
Left anterior cingulate	BA32	0	44	12	3.23	.999			
Left superior frontal gyrus	BA10	-26	42	30	3.19	1.000			
Left medial frontal gyrus	BA10	-2	58	-4	3.17	1.000			
Left inferior parietal lobule	BA40	-54	-22	26	3.16	1.000			
Left transverse temporal gyrus	BA41	-48	-26	10	3.16	1.000			
Left postcentral gyrus	BA40	-48	-34	54	3.73	.878			
Left inferior parietal lobule	BA40	-36	-52	56	3.54	.968	231	.035	.586
Left inferior temporal gyrus	BA20	-64	-8	-26	3.32	.998			
Left fusiform gyrus	BA20	-62	-4	-28	3.20	1.000			
Left middle temporal gyrus	BA21	-54	0	-18	2.84	1.000	262	.026	.482
Right inferior frontal gyrus	BA47	42	14	-14	3.32	.998			
Right superior temporal gyrus	BA22	46	0	-4	3.16	1.000			
Right subgyral	BA13	44	2	-8	3.08	1.000			
Right insula	BA13	42	-6	4	2.92	1.000			

Abbreviations: PiB, Pittsburgh compound B; APOE , apolipoprotein E; $\text{A}\beta$, amyloid beta; $P_{\text{FWE-corr}}$, voxel-level P -value after familywise error correction; k , number of voxels in cluster; P_{uncorr} , cluster-level uncorrected P -value; P_{corr} , cluster-level P -value after random field theory correction; BA, Brodmann area.

found a difference in peripheral $\text{A}\beta$ clearance from the plasma by APOE genotype. The results suggested that $\text{APOE } \epsilon 4$ gene expression results in a protein (apoE4) with lowered efficiency of peripheral $\text{A}\beta$ clearance from the plasma. Tight junction integrity in the BBB is also regulated by the apoE protein in an isoform-dependent manner, with impaired tight junction integrity and increased BBB permeability observed in mice with the apoE4 isoform compared with mice with expression of the apoE3 isoform [26]. Thus, reduced $\text{A}\beta$ clearance by apoE4 protein may lead to an impaired BBB, which in turn affects $\text{A}\beta$ levels in the brain and plasma, and the relationship between these compartments.

Binding of the apoE protein to $\text{A}\beta$ may also influence $\text{A}\beta$ clearance from the brain into the plasma. The apoE protein binds strongly to $\text{A}\beta$, but the binding characteristics of the apoE4 isoform are different than those of the apoE3 isoform [42,43]. Oxidized apoE4 binds more rapidly to synthetic $\text{A}\beta$ than oxidized apoE3. Binding by oxidized apoE4 was also more sensitive to pH changes than oxidized apoE3. In addition, the $\text{APOE } \epsilon 4$ allele is associated with increased vascular and plaque amyloid deposits [44]. $\text{APOE } \epsilon 4$ homozygotes have more amyloid deposits in the vasculature and tissue compared with $\text{APOE } \epsilon 3$ homozygotes. $\text{APOE } \epsilon 3/\epsilon 4$ heterozygotes have intermediate amyloid deposits. In a recent study, free

apoE protein was shown to facilitate a greater removal of $\text{A}\beta$ from the brain into the periphery across the BBB compared with apoE protein bound to $\text{A}\beta$ [45]. Furthermore, apoE isoform-specific differences were observed in $\text{A}\beta$ transport. Specifically, $\text{A}\beta$ bound to the apoE4 isoform had increased blood-to-brain transport when compared with $\text{A}\beta$ bound to the apoE3 isoform. The authors found that the apoE4 isoform had decreased $\text{A}\beta$ clearance across the BBB in comparison with the apoE3 isoform. More recently, Bachmeier et al. [46] observed that retinoid X receptor stimulation increased $\text{A}\beta$ clearance across the BBB, an effect that was believed to be partially mediated by the apoE protein.

The apoE protein has been shown to be present in greater amounts in the AD brain relative to those of healthy elders. Furthermore, apoE undergoes significantly more cleavage in the AD brain than in HCs, especially in $\text{APOE } \epsilon 4$ carriers [47]. The N-terminal domain of the apoE protein contains the major receptor-binding region; the C-terminal domain contains the lipid-binding region. The C-terminal domain of both the apoE3 and apoE4 isoforms has been shown to interact closely with $\text{A}\beta$ [47]. Isolated C-terminal-truncated apoE4 protein fragments have been shown to be associated with $\text{A}\beta$ plaques [47]. Last, inefficient clearance of $\text{A}\beta$ peptides produces neuronal and behavioral deficits in mice [48]. Thus, differential clearance of $\text{A}\beta$ by the apoE protein

isoform, which is coded for by different *APOE* genotypes, may be a potential explanation for the *APOE* genotype effects observed in the current study. Further investigation of mechanistic explanations is warranted.

It is important to discuss the limitations of the current study. First, the sample size in this study was relatively modest, as only 96 participants in the ADNI cohort had both [¹¹C] PiB PET scans and concomitant plasma measurements of Aβ_{1–40} and Aβ_{1–42}. Our results suggest a complex relationship between plasma Aβ, brain Aβ, and *APOE* genotype, warranting further investigation in independent and larger samples. Second, a majority of the participants (n = 52) in the current study had a diagnosis of MCI. Therefore, it is possible that the observed association may have been driven primarily by these participants. Because of the relatively small number of participants in the three diagnostic groups, we were unable to perform analyses within each diagnostic group to determine whether there was an effect of diagnosis. Last, genetic factors other than *APOE* may also play a role in modulating the association of plasma and brain Aβ. Investigation of the impact of other known and novel AD-associated genetic variants on the relationship between plasma and brain Aβ represents a possible future direction of this work.

5. Summary

In summary, we detected an association between soluble plasma Aβ and fibrillar brain Aβ that was modulated by *APOE* ε4 status. Replication and additional study in independent samples is needed to clarify the nature of this interaction as well as to understand the underlying biological mechanisms. Our results suggest that plasma Aβ levels have great potential as an AD biomarker, and emphasize the importance of genetic variation in the interpretation of plasma Aβ levels.

Acknowledgments

Data collection and sharing for this project was funded by the Alzheimer's Disease Neuroimaging Initiative (ADNI) National Institutes of Health (NIH) grant U01AG024904; RC2AG036535. ADNI is funded by the National Institute on Aging (NIA), the National Institute of Biomedical Imaging and Bioengineering, and through generous contributions from the following: Abbott; Alzheimer's Association; Alzheimer's Drug Discovery Foundation; Amorfis Life Sciences Ltd.; AstraZeneca; Bayer HealthCare; BioClinica, Inc.; Biogen Idec, Inc.; Bristol-Myers Squibb Company; Eisai, Inc.; Elan Pharmaceuticals, Inc.; Eli Lilly and Company; F. Hoffmann-La Roche Ltd and its affiliated company Genentech, Inc.; GE Healthcare; Innogenetics, N.V.; IXICO Ltd.; Janssen Alzheimer Immunotherapy Research & Development, LLC.; Johnson & Johnson Pharmaceutical Research & Development LLC.; Medpace, Inc.; Merck & Co., Inc.; Meso Scale Diagnostics, LLC; Novartis Pharmaceuticals Corporation; Pfizer,

Inc.; Servier; Synarc, Inc.; and Takeda Pharmaceutical Company. The Canadian Institutes of Health Research is providing funds to support ADNI clinical sites in Canada. Private-sector contributions are facilitated by the Foundation for the National Institutes of Health (www.fnih.org). The grantee organization is the Northern California Institute for Research and Education, and the study is coordinated by the Alzheimer's Disease Cooperative Study at the University of California at San Diego. ADNI data are disseminated by the Laboratory for Neuro Imaging at the University of California at Los Angeles. This research was also supported by NIH grants (P30AG010129, K01AG030514), the Dana Foundation, U01AG032984 Alzheimer's Disease Genetics Consortium grant, NIA R01AG19771, P30AG010133, the Indiana Economic Development Corporation (IEDC no. 87884), and the Foundation for the National Institutes of Health for data analysis. We also thank the following people: genotyping at TGen: Matthew Huentelman, PhD, and David Craig, PhD; sample processing, storage, and distribution at the National Cell Repository for Alzheimer's Disease (NCRAD): Kelley Faber and Colleen Mitchell. Samples from the NCRAD, which receives government support under a cooperative agreement (U24AG021886) awarded by the NIA were used in this study. We thank contributors who collected samples as well as patients and their families, whose participation and help made this work possible.

RESEARCH IN CONTEXT

1. Systematic review: Our scientific issue was to determine the influence of apolipoprotein E (*APOE*) ε4 status on the relationship between soluble plasma amyloid beta (Aβ) and fibrillar brain Aβ measured by Pittsburgh compound B ([¹¹C]PiB) positron emission tomography. We performed a literature search and identified four studies that had investigated the relationship between plasma Aβ and brain Aβ measured by [¹¹C]PiB, but did not examine the role of *APOE* ε4 on modulating the relationship.
2. Interpretation: A positive relationship between plasma Aβ and [¹¹C]PiB uptake was observed in *APOE* ε4– participants, but not *APOE* ε4+ participants. The findings suggests the utility of plasma Aβ as a potential Alzheimer's disease biomarker and highlight the importance of genetic variation in interpretation of plasma Aβ levels.
3. Future directions: Replication and additional study in independent samples is needed to determine the biological mechanisms that can explain the findings. The role of other genetic factors should also be investigated.

References

- [1] Alzheimer's Association. 2012 Alzheimer's disease facts and figures. *Alzheimers Dement* 2012;8:131–68.
- [2] Hampel H, Frank R, Broich K, Teipel SJ, Katz RG, Hardy J, et al. Biomarkers for Alzheimer's disease: academic, industry and regulatory perspectives. *Nat Rev Drug Discov* 2010;9:560–74.
- [3] Petersen RC, Smith GE, Waring SC, Ivnik RJ, Tangalos EG, Kokmen E. Mild cognitive impairment: clinical characterization and outcome. *Arch Neurol* 1999;56:303–8.
- [4] Albert MS, DeKosky ST, Dickson D, Dubois B, Feldman HH, Fox NC, et al. The diagnosis of mild cognitive impairment due to Alzheimer's disease: recommendations from the National Institute on Aging–Alzheimer's Association workgroups on diagnostic guidelines for Alzheimer's disease. *Alzheimers Dement* 2011;7:270–9.
- [5] Shaw LM, Vanderstichele H, Knapik-Czajka M, Clark CM, Aisen PS, Petersen RC, et al. Cerebrospinal fluid biomarker signature in Alzheimer's Disease Neuroimaging Initiative subjects. *Ann Neurol* 2009;65:403–13.
- [6] Okonkwo OC, Mielke MM, Griffith HR, Moghekar AR, O'Brien RJ, Shaw LM, et al. Cerebrospinal fluid profiles and prospective course and outcome in patients with amnesic mild cognitive impairment. *Arch Neurol* 2011;68:113–9.
- [7] Buchhave P, Minthon L, Zetterberg H, Wallin AK, Blennow K, Hansson O. Cerebrospinal fluid levels of beta-amyloid 1–42, but not of tau, are fully changed already 5 to 10 years before the onset of Alzheimer dementia. *Arch Gen Psychiatry* 2012;69:98–106.
- [8] Rabinovici GD, Jagust WJ. Amyloid imaging in aging and dementia: testing the amyloid hypothesis in vivo. *Behav Neurol* 2009;21:117–28.
- [9] Choi SR, Schneider JA, Bennett DA, Beach TG, Bedell BJ, Zehntner SP, et al. Correlation of amyloid PET ligand florbetapir F 18 binding with Abeta aggregation and neuritic plaque deposition in postmortem brain tissue. *Alzheimer Dis Assoc Disord* 2012;26:8–16.
- [10] Clark CM, Schneider JA, Bedell BJ, Beach TG, Bilker WB, Mintun MA, et al. Use of florbetapir-PET for imaging beta-amyloid pathology. *JAMA* 2011;305:275–83.
- [11] Jack CR Jr, Lowe VJ, Senjem ML, Weigand SD, Kemp BJ, Shiung MM, et al. 11C PiB and structural MRI provide complementary information in imaging of Alzheimer's disease and amnesic mild cognitive impairment. *Brain* 2008;131:665–80.
- [12] Klunk WE, Engler H, Nordberg A, Wang Y, Blomqvist G, Holt DP, et al. Imaging brain amyloid in Alzheimer's disease with Pittsburgh compound-B. *Ann Neurol* 2004;55:306–19.
- [13] Wong DF, Rosenberg PB, Zhou Y, Kumar A, Raymont V, Ravert HT, et al. In vivo imaging of amyloid deposition in Alzheimer disease using the radioligand 18F-AV-45 (florbetapir [corrected] F 18). *J Nucl Med* 2010;51:913–20.
- [14] Mayeux R, Schupf N. Blood-based biomarkers for Alzheimer's disease: plasma Abeta40 and Abeta42, and genetic variants. *Neurobiol Aging* 2011;32:S10–9.
- [15] Song F, Poljak A, Valenzuela M, Mayeux R, Smythe GA, Sachdev PS. Meta-analysis of plasma amyloid-beta levels in Alzheimer's disease. *J Alzheimers Dis* 2011;26:365–75.
- [16] Koyama A, Okereke OI, Yang T, Blacker D, Selkoe DJ, Grodstein F. Plasma amyloid-beta as a predictor of dementia and cognitive decline: a systematic review and meta-analysis. *Arch Neurol* 2012;69:824–31.
- [17] Thambisetty M, Lovestone S. Blood-based biomarkers of Alzheimer's disease: challenging but feasible. *Biomark Med* 2010;4:65–79.
- [18] Corder EH, Saunders AM, Strittmatter WJ, Schmechel DE, Gaskell PC, Small GW, et al. Gene dose of apolipoprotein E type 4 allele and the risk of Alzheimer's disease in late onset families. *Science* 1993;261:921–3.
- [19] Saunders AM, Strittmatter WJ, Schmechel D, George-Hyslop PH, Pericak-Vance MA, Joo SH, et al. Association of apolipoprotein E allele epsilon 4 with late-onset familial and sporadic Alzheimer's disease. *Neurology* 1993;43:1467–72.
- [20] Farrer LA, Cupples LA, Haines JL, Hyman B, Kukull WA, Mayeux R, et al. Effects of age, sex, and ethnicity on the association between apolipoprotein E genotype and Alzheimer disease: a meta-analysis: APOE and Alzheimer Disease Meta Analysis Consortium. *JAMA* 1997;278:1349–56.
- [21] Reiman EM, Chen K, Liu X, Bandy D, Yu M, Lee W, et al. Fibrillar amyloid-beta burden in cognitively normal people at 3 levels of genetic risk for Alzheimer's disease. *Proc Natl Acad Sci U S A* 2009;106:6820–5.
- [22] Toledo JB, Vanderstichele H, Figurski M, Aisen PS, Petersen RC, Weiner MW, et al. Factors affecting Abeta plasma levels and their utility as biomarkers in ADNI. *Acta Neuropathol* 2011;122:401–13.
- [23] Donahue JE, Johanson CE. Apolipoprotein E, amyloid-beta, and blood–brain barrier permeability in Alzheimer disease. *J Neuropathol Exp Neurol* 2008;67:261–70.
- [24] Castellano JM, Kim J, Stewart FR, Jiang H, DeMattos RB, Patterson BW, et al. Human apoE isoforms differentially regulate brain amyloid-beta peptide clearance. *Sci Transl Med* 2011;3: 89ra57.
- [25] Sharman MJ, Morici M, Hone E, Berger T, Taddei K, Martins LJ, et al. APOE genotype results in differential effects on the peripheral clearance of amyloid-beta42 in APOE knock-in and knock-out mice. *J Alzheimers Dis* 2010;21:403–9.
- [26] Nishitsuji K, Hosono T, Nakamura T, Bu G, Michikawa M. Apolipoprotein E regulates the integrity of tight junctions in an isoform-dependent manner in an in vitro blood–brain barrier model. *J Biol Chem* 2011;286:17536–42.
- [27] Fagan AM, Mintun MA, Mach RH, Lee SY, Dence CS, Shah AR, et al. Inverse relation between in vivo amyloid imaging load and cerebrospinal fluid Abeta42 in humans. *Ann Neurol* 2006;59:512–9.
- [28] Lui JK, Laws SM, Li QX, Villemagne VL, Ames D, Brown B, et al. Plasma amyloid-beta as a biomarker in Alzheimer's disease: the AIBL study of aging. *J Alzheimers Dis* 2010;20:1233–42.
- [29] Devanand DP, Schupf N, Stern Y, Parsey R, Pelton GH, Mehta P, et al. Plasma Abeta and PET PiB binding are inversely related in mild cognitive impairment. *Neurology* 2011;77:125–31.
- [30] Weiner MW, Aisen PS, Jack CR Jr, Jagust WJ, Trojanowski JQ, Shaw L, et al. The Alzheimer's Disease Neuroimaging Initiative: progress report and future plans. *Alzheimers Dement* 2010;6:202–11.
- [31] Jagust WJ, Landau SM, Shaw LM, Trojanowski JQ, Koeppe RA, Reiman EM, et al. Relationships between biomarkers in aging and dementia. *Neurology* 2009;73:1193–9.
- [32] Jagust WJ, Bandy D, Chen K, Foster NL, Landau SM, Mathis CA, et al. The Alzheimer's Disease Neuroimaging Initiative positron emission tomography core. *Alzheimers Dement* 2010;6:221–9.
- [33] Friston KJ, Holmes AP, Worsley KJ, Poline JP, Frith CD, Frackowiak RSJ. Statistical parametric maps in functional imaging: a general linear approach. *Hum Brain Mapp* 1994;2:189–210.
- [34] Swaminathan S, Shen L, Risacher SL, Yoder KK, West JD, Kim S, et al. Amyloid pathway-based candidate gene analysis of [(11)C] PiB-PET in the Alzheimer's Disease Neuroimaging Initiative (ADNI) cohort. *Brain Imaging Behav* 2012;6:1–15.
- [35] Jack CR Jr, Bernstein MA, Fox NC, Thompson P, Alexander G, Harvey D, et al. The Alzheimer's Disease Neuroimaging Initiative (ADNI): MRI methods. *J Magn Reson Imaging* 2008;27:685–91.
- [36] Risacher SL, Saykin AJ, West JD, Shen L, Firpi HA, McDonald BC, et al. Baseline MRI predictors of conversion from MCI to probable AD in the ADNI cohort. *Curr Alzheimer Res* 2009;6:347–61.
- [37] Figurski MJ, Waligorska T, Toledo J, Vanderstichele H, Korecka M, Lee VM, et al. Improved protocol for measurement of plasma beta-amyloid in longitudinal evaluation of Alzheimer's Disease Neuroimaging Initiative study patients. *Alzheimers Dement* 2012; 8:250–60.
- [38] Saykin AJ, Shen L, Foroud TM, Potkin SG, Swaminathan S, Kim S, et al. Alzheimer's Disease Neuroimaging Initiative biomarkers as quantitative phenotypes: genetics core aims, progress, and plans. *Alzheimers Dement* 2010;6:265–73.

- [39] R Core Team. R: a language and environment for statistical computing. Vienna, Austria: R Foundation for Statistical Computing; 2012.
- [40] Lancaster JL, Rainey LH, Summerlin JL, Freitas CS, Fox PT, Evans AC, et al. Automated labeling of the human brain: a preliminary report on the development and evaluation of a forward-transform method. *Hum Brain Mapp* 1997;5:238–42.
- [41] Lancaster JL, Woldorff MG, Parsons LM, Liotti M, Freitas CS, Rainey L, et al. Automated Talairach atlas labels for functional brain mapping. *Hum Brain Mapp* 2000;10:120–31.
- [42] Strittmatter WJ, Saunders AM, Schmechel D, Pericak-Vance M, Enghild J, Salvesen GS, et al. Apolipoprotein E: high-avidity binding to beta-amyloid and increased frequency of type 4 allele in late-onset familial Alzheimer disease. *Proc Natl Acad Sci U S A* 1993; 90:1977–81.
- [43] Strittmatter WJ, Weisgraber KH, Huang DY, Dong LM, Salvesen GS, Pericak-Vance M, et al. Binding of human apolipoprotein E to synthetic amyloid beta peptide: isoform-specific effects and implications for late-onset Alzheimer disease. *Proc Natl Acad Sci U S A* 1993; 90:8098–102.
- [44] Schmechel DE, Saunders AM, Strittmatter WJ, Crain BJ, Hulette CM, Joo SH, et al. Increased amyloid beta-peptide deposition in cerebral cortex as a consequence of apolipoprotein E genotype in late-onset Alzheimer disease. *Proc Natl Acad Sci U S A* 1993;90:9649–53.
- [45] Bachmeier C, Paris D, Beaulieu-Abdelahad D, Mouzon B, Mullan M, Crawford F. A multifaceted role for apoE in the clearance of beta-amyloid across the blood–brain barrier. *Neurodegener Dis* 2013; 11:13–21.
- [46] Bachmeier C, Beaulieu-Abdelahad D, Crawford F, Mullan M, Paris D. Stimulation of the retinoid X receptor facilitates beta-amyloid clearance across the blood–brain barrier. *J Mol Neurosci* 2013;49:270–6.
- [47] Jones PB, Adams KW, Rozkalne A, Spires-Jones TL, Hshieh TT, Hashimoto T, et al. Apolipoprotein E: isoform specific differences in tertiary structure and interaction with amyloid-beta in human Alzheimer brain. *PLoS One* 2011;6:e14586.
- [48] Bien-Ly N, Andrews-Zwilling Y, Xu Q, Bernardo A, Wang C, Huang Y. C-terminal-truncated apolipoprotein (apo) E4 inefficiently clears amyloid-beta (Aβ) and acts in concert with Aβ to elicit neuronal and behavioral deficits in mice. *Proc Natl Acad Sci U S A* 2011;108:4236–41.